

## Metabolic adaptations to chronic glucose infusion in rats

B. G. Topp<sup>1</sup> · M. D. McArthur<sup>1</sup> · D. T. Finegood<sup>1</sup>

<sup>1</sup> Diabetes Research Laboratory, School of Kinesiology, Simon Fraser University, Burnaby, British Columbia, Canada

### Abstract

*Aims/hypothesis.* Several studies have employed the chronic glucose infusion protocol to quantify the metabolic adaptations associated with a prolonged glucose challenge. However, the limited number of indices and time points reported by these studies has generated an incomplete picture of this process. In this study we aimed to generate an integrative and dynamic picture of the physiological adaptations that occur during chronic glucose infusion.

*Methods.* Sprague–Dawley rats were infused with either 50% dextrose or saline (2 ml/h) for a period of between 0 and 6 days. Glucose, insulin and NEFA dynamics were determined from daily blood samples. Subsets of animals were killed daily for histological determination of beta cell mass, size and replication rates. The mathematical model of coupled beta cell mass, insulin and glucose (the  $\beta$ IG model) was used to estimate insulin sensitivity, beta cell function and net neogenesis from this data.

*Results.* Glucose-infused rats displayed transient hyperglycaemia, persistent hyperinsulinaemia and un-

changed NEFA levels. Insulin sensitivity decreased by approximately 80% during the first day of glucose infusion, but had returned to pre-infusion levels by Day 3. Beta cell function was four to six times higher than in control rats throughout the experiment. Beta cell mass doubled over the 6 days of glucose infusion due to three phases of adaptation: (i) neogenesis; (ii) hypertrophy and hyperplasia; and (iii) continued hyperplasia coupled to a second wave of neogenesis.

*Conclusions/interpretation.* Contrary to the results reported for perfused pancreas and in vitro experiments, we found that chronic glucose infusion elevated beta cell function. The prediction of a second wave of beta cell neogenesis, coupled with our previous report of “focal areas” on Day 3, suggests the existence of delayed acinar-to-islet transdifferentiation.

**Keywords** Beta cell function · Beta cell mass · Diabetes mellitus · Glucose infusion · Insulin sensitivity · Islets of Langerhans · Mathematical modelling

Received: 6 January 2004 / Accepted: 14 May 2004

Published online: 2 September 2004

© Springer-Verlag 2004

D. T. Finegood (✉)  
Diabetes Research Laboratory, School of Kinesiology,  
Simon Fraser University, 8888 University Drive, Burnaby,  
British Columbia, Canada V5A 1S6  
E-mail: finegood@sfu.ca  
Tel.: +1-604-2913319, Fax: +1-604-2913040

### Introduction

Since its first application in the 1980s [1], chronic high-dose glucose infusion has been used to quantify the effects of increased glucose supply on insulin sen-

*Abbreviations:*  $\beta$ IG model, model of beta cell mass, insulin and glucose · BrdU, 5-bromo-2'-deoxyuridine · DAB, 3,3'-diaminobenzidine tetrahydrochloride · HOMA, homeostasis model assessment · QUICKI, quantitative insulin sensitivity check index · TUNEL, terminal deoxynucleotidyl transferase nick end-labelling

sitivity [2, 3, 4], beta cell function [5, 6, 7, 8, 9], beta cell mass [6, 10, 11] and indices of beta cell replication [10, 11], death [10] and neogenesis [10]. However, the limited number of variables and time points presented in these studies has led to an incomplete understanding of this process. For example, hyperglycaemia has long been known to induce insulin resistance in muscle. However, recent studies have shown that prolonged glucose infusion leads to augmented insulin action in adipose tissue [3, 4]. The time course and sustainability of this adaptation remains unclear. Also, several *in vitro* and *in situ* studies have suggested that beta cell function is impaired by chronic glucose infusion, while *in vivo* acute insulin response studies have provided conflicting results [5, 6, 7, 8]. Finally, while several studies have reported morphological evidence of neogenesis, apoptosis or transdifferentiation, it is unclear whether changes in these markers reflect significant contributions of these processes to the observed beta-cell-mass dynamics [6, 10, 11].

Existing studies tend to focus on only one of the following: insulin resistance, beta cell function or beta cell mass. This is based partly on the time, expense and expertise associated with existing *in vivo* methodologies such as the hyperinsulinaemic clamp, perfusion of the pancreas and quantitative histology. The same factors also explain the limited number of time points typically reported in these studies. The relative contributions of death and neogenesis to overall beta-cell-mass dynamics cannot be quantified due to an incomplete understanding of the time taken for a labelled cell to progress from one stage to another (i.e. alive to engulfed or duct cell, or acinar cell to beta cell). Taken together, these limitations suggest that novel *in vivo* methodologies or data analysis techniques need to be developed if a truly integrative and dynamical analysis of this process is to be obtained.

While advancements in longitudinal *in vivo* imaging techniques hold great potential for the indirect assessment of cellular population sizes or gene transcription rates, mathematical modelling has already been used to indirectly assess metabolic processes from easily obtained experimental data. Examples of this include the homeostasis model assessment (HOMA) [12] and the quantitative insulin sensitivity check index (QUICKI) [13], which have widely been used to estimate insulin sensitivity and/or beta cell function from fasting glucose and insulin levels. In addition to the indirect assessment of metabolic indices, mathematical modelling has been used to generate indices that cannot be determined histologically, such as rates of beta cell death or neogenesis *in vivo* [14]. We recently developed a mathematical model that coupled the dynamics of beta cell mass, insulin and glucose (the  $\beta$ IG model). Although this was initially designed as a bifurcation and simulation analysis tool, we found that the  $\beta$ IG model could also be

used to generate indirect estimates of insulin sensitivity, beta cell function and net beta cell neogenesis [15]. These indices have been shown to correlate strongly with indices derived from the Minimal model and from HOMA in a large human data set covering the entire range of glucose tolerance (data not shown). However, unlike the HOMA, QUICKI and Minimal models, the  $\beta$ IG model can be easily re-fitted with species-specific parameter values and applied to *in vivo* data.

The aim of this study was to perform an integrative and dynamic analysis of the metabolic adaptations to chronic glucose infusion by using the  $\beta$ IG model to generate daily estimates of insulin sensitivity, beta cell function and net neogenesis from experimental data obtained in Sprague–Dawley rats infused with 50% dextrose or saline over a period of between 0 and 6 days.

## Materials and methods

**Animals.** The infusion protocol used was similar to that of Bonner-Weir et al. [11]. Male Sprague–Dawley rats (weight ~230 g) were housed in plastic shoebox cages at 22 °C, with a light–dark cycle of 12 h each, and had free access to food and water. Under anaesthesia (sodium pentobarbital, 35 mg/kg *i.p.*), each rat was fitted with an indwelling jugular catheter (Intramedic PE50; Becton Dickinson, Sparks, Md., USA), which was exteriorised at the nape of the neck and connected by flexible tether to a swivel system. The tethers were attached to lightweight stretch cotton vests that were custom-made to fit the rats, allowing for free movement within the cage. All procedures were performed in accordance with the standards of the Canadian Council on Animal Care and were approved by the Health Sciences Animal Welfare Committee at the University of Alberta (Edmonton, Alta, Canada) and the Animal Care Committee of Simon Fraser University (Burnaby, BC, Canada).

During recovery from surgery, catheter patency was maintained by a slow infusion of 0.9% saline. After 3 to 5 days, rats were either killed (Day 0,  $n=10$ ) or infused (2 ml/h) with 0.45% saline ( $n=40$ ) or 50% dextrose in 0.45% saline ( $n=65$ ) for 1, 2, 3, 4, 5 or 6 days. Blood samples were taken daily from the tail vein. Animals were allowed free access to regular chow and water during the infusion period. On the final infusion day, 6 h before the animals were killed, each rat was injected with 100 mg/kg of 5-bromo-2'-deoxyuridine (BrdU; Amersham Canada, Oakville Ont, Canada), a thymidine analogue which is incorporated into newly synthesised DNA. At the time of killing, rats were anaesthetised (sodium pentobarbital 35 mg/kg *i.p.*) and a blood sample was taken by cardiac puncture. The pancreas was rapidly excised and dissected free from surrounding connective and adipose tissue. Each pancreas was cut into three pieces, which were then blotted, weighed and placed in separate cassettes. The tissue was fixed overnight in Bouin's solution, washed for 8 h in cold running water and then stored in 10% buffered formalin before being embedded in paraffin.

**Plasma assays.** Blood samples were kept on ice prior to centrifugation to recover plasma. Plasma was stored at –20 °C until assayed. Plasma glucose was measured by the glucose oxidase method (Trinder kit; Sigma Diagnostics, St. Louis, Mo., USA) on duplicate 5- $\mu$ l samples using a microplate reader. Plasma NEFA were determined using an enzymatic colorimetric method (ACS-ACOD; Wako Chemicals USA, Rich-

mond, Va., USA) on duplicate 4- $\mu$ l samples using the microplate reader. Plasma insulin was assayed by RIA using a specific anti-rat-insulin antibody and rat insulin standards (Linco Research, St. Louis, Mo., USA). The detection limit was 0.1 ng/ml, and the intra-assay and inter-assay coefficients of variation were lower than 10%.

**Immunocytochemistry.** Sections (4–5  $\mu$ m thick) from each of the three pieces of pancreas were de-waxed in xylene. Endogenous peroxidase activity was blocked with 0.3% hydrogen peroxide. After washing in PBS, the sections were incubated with 10% lamb serum in PBS for 30 min at room temperature. The slides used for determination of beta cell mass and size were stained with a cocktail of antibodies to glucagon, somatostatin and pancreatic polypeptide (rabbit anti-human, 1:2000 dilution; Dako Diagnostics Canada, Mississauga, Ont, Canada) for identification of islet non-beta cells (alpha, delta, PP cells). The slides used for determination of beta cell replication were double-stained with the antibody cocktail and anti-BrdU antibody (mouse monoclonal anti-BrdU, 1:100 dilution; Amersham Canada). The slides were incubated with primary antibodies overnight at 4 °C before being washed in PBS and incubated with the secondary antibodies (biotinylated goat anti-guinea pig IgG, biotinylated goat anti-mouse IgG or biotinylated goat anti-rabbit IgG, 1:500 dilution; Dako Diagnostics, Canada) for 1 h at room temperature. Sections were then washed in PBS, incubated with avidin–biotin complexed with horseradish peroxidase (1:1000 dilution; Vectastain Elite ABC Kit, Vector Laboratories Canada, Burlington, Ont, Canada) for 1 h and then developed using 3,3'-diaminobenzidine tetrahydrochloride (DAB; Sigma-Aldrich Canada, Oakville, Ont, Canada). All slides were counterstained with Meyers haematoxylin (Sigma-Aldrich).

**Determination of beta cell mass.** Beta cell mass was determined from antibody-cocktail-stained sections using an image analysis system. This system consisted of an Olympus light microscope (Model BX40, Carsen Group, Markham, Ont, Canada) attached to Sony colour video camera (Model DXC-950, Sony, Tokyo, Japan) and Northern Eclipse software (Empix Imaging, Mississauga, Ont, Canada). Each section was stepped through in 1.5 $\times$ 1.5-mm stage increments (at 400 $\times$  magnification). For each field, the areas corresponding to pancreas (exocrine and endocrine), non-pancreas (fat, space, connective tissue) and islet (beta cells and non-beta cells) were determined. Total islet area was determined by hand-tracing each islet perimeter identified by the mantle of non-beta cells and the morphology of the tissue. Non-beta cell area was determined by distinguishing DAB-stained tissue within the hand-traced region of interest using the threshold function of the image analysis software. Beta cell area was calculated as the difference between total islet area and non-beta cell area. Islet area relative to total tissue area was determined by using the threshold function to quantify total tissue area stained with haematoxylin and DAB in each field. For fields containing adipose tissue, the area of “white space” previously occupied by lipid was determined separately and added to the total tissue area. Beta cell mass was calculated as the relative area of tissue occupied by beta cells multiplied by the wet weight of pancreas segment. Data from individual portions of each pancreas were summed.

**Determination of beta cell size.** Measurements of individual beta cell area were made in islets with ten or more beta cells, since significantly greater measurement error was associated with smaller islets (data not shown). Antibody-cocktail-stained sections were scanned and every islet with ten or more beta cells was assessed for beta cell size. Beta cell area was determined as described above by hand-tracing the islet perimeter

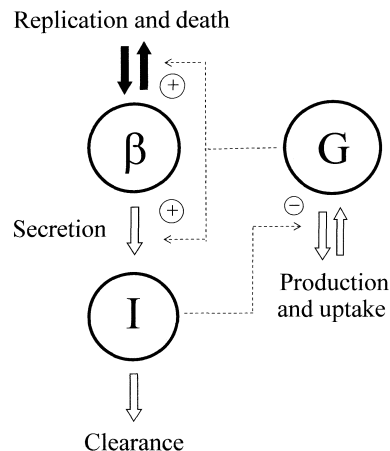


**Fig. 1.** The  $\beta$ IG mathematical model of coupled beta cell mass ( $\beta$ ), insulin (I) and glucose (G) dynamics. Glucose regulates blood insulin levels by increasing insulin secretion rates over a fast time scale, and by augmenting beta cell replication and death rates over a slower time scale. +, positive feedback; –, negative feedback

and “thresholding” for non-beta cells stained by cocktail. The number of nuclei in the beta cell area was counted and the average cross-sectional area of a single beta cell was calculated as the total beta cell area divided by the number of nuclei. This method has been shown to overestimate average beta cell size compared with electron microscope determinations, but is considered acceptable for comparison of treatment effects [10, 16]. Beta cell volume was estimated from the cross-sectional area based on the calculated radius (area =  $\pi r^2$ ) and the volume of a sphere (volume =  $4/3\pi r^3$ ). The average beta cell size (in  $\mu$ g) is represented by the symbol  $\beta_s$ .

**Determination of beta cell replication.** Sections double-stained with antibody cocktail and anti-BrdU antibody were used to assess beta cell replication. BrdU incorporation was determined by systematically sampling all of the beta cells in each section that were identified with cocktail staining, using a light microscope under high magnification ( $\times$ 1000). Beta cells incorporating BrdU (BrdU-positive) had blue/black nuclei.

**$\beta$ IG model estimates of insulin sensitivity, beta cell function and net-neogenesis.** A schematic diagram of the  $\beta$ IG-model feedback loops is shown in Figure 1. Details of the  $\beta$ IG model data analysis can be found in the appendix.

**Statistical analysis.** Data are presented as means  $\pm$  SEM unless stated otherwise. For the measured variables (glucose, insulin, beta cell mass, BrdU incorporation, beta cell cross-sectional area), the effect of treatment (saline vs glucose infusion) and time were determined by analysis of variance with Tukey–Kraemer post-hoc tests. Unless otherwise stated, a *p* value of less than 0.05 was considered significant. All statistical calculations were performed using SAS, Version 7.0 (SAS Institute, Cary, N.C., USA).

## Results

**Body and pancreas weight.** Body weight and pancreatic weight data are presented in Table 1. Except for Day 4 of infusion, body weight did not differ between the

**Table 1.** Body weight and pancreatic weight of saline- and glucose-infused rats

Variable	Infusion day	Saline-infused rats	n	Glucose-infused rats	n
Body weight (g)	0	235.6±4.4	10		
	1	224.9±4.1	7	228.9±6.7	10
	2	236.8±6.8	6	232.4±5.9	10
	3	242.7±9.7	8	251.5±7.7	18
	4	246.1±5.1	9	231.1±3.0 <sup>b</sup>	13
	5	264.6±6.0 <sup>a</sup>	6	274.1±7.0 <sup>a</sup>	8
	6	262.3±4.8	4	267.7±9.9	5
Pancreas weight (mg)	0	1176.3±128.7	10		
	1	916.9±31.7	7	725.6±33.4 <sup>a, b</sup>	10
	2	993.8±29.9	6	761.1±43.7 <sup>a, b</sup>	10
	3	1072.9±33.4	8	804.8±31.8 <sup>a, b</sup>	18
	4	980.6±41.2	9	701.0±22.2 <sup>a</sup>	13
	5	1147.7±79.0	6	900.3±47.8 <sup>a, b</sup>	8
	6	1128.5±53.0	4	722.8±66.6 <sup>a, b</sup>	5

Values are shown as means ± SEM. <sup>a</sup>  $p < 0.05$  vs Day 0; <sup>b</sup>  $p < 0.05$  vs saline-infused animals

saline-infused group and the glucose-infused group. While there was a general tendency for the animals to gain weight with increasing length of infusion of either type, this was only significant on Day 5 of infusion and may be due in part to differences between groups prior to surgery (data not shown). Pancreas mass was approximately 35% lower in glucose-infused rats than in saline-infused rats on all infusion days except Day 5 (Table 1).

**Plasma data.** Saline infusion led to a slight (~15%) reduction in plasma glucose levels, but had no effect on plasma insulin concentrations (Fig. 2). The NEFA concentration tended to increase with time in saline-infused animals. The glucose-infused animals displayed marked hyperglycaemia on Day 1 and Day 2 of infusion. Glucose returned to pre-infusion levels by Day 3 and remained low throughout the remainder of the study. Insulin levels increased from  $180 \pm 12$  to  $2256 \pm 306$  pmol/l during the first day of infusion and decreased to  $1476 \pm 792$  pmol/l by Day 5 (Fig. 2). NEFA levels rose on Day 1 then returned to baseline levels by Day 2 and thus tended to be lower than levels observed in saline-infused animals. It should be noted that glucose and insulin dynamics were derived from tail-vein blood samples while NEFA levels were determined from cardiac puncture blood samples that were taken at the time that the animals were killed. Tail-vein blood samples were not taken on the day the animals were killed; consequently, neither glucose nor insulin data are available for Day 6 of infusion.

**Histological analysis of pancreas.** Saline infusion did not affect beta cell mass or individual beta cell size; however, it did have a small but significant negative effect on BrdU incorporation on Day 3 and Day 5 of infusion. Conversely, glucose-infused animals displayed an approximately linear two-fold increase in beta cell mass (from  $5.1 \pm 0.3$  mg on Day 0 to

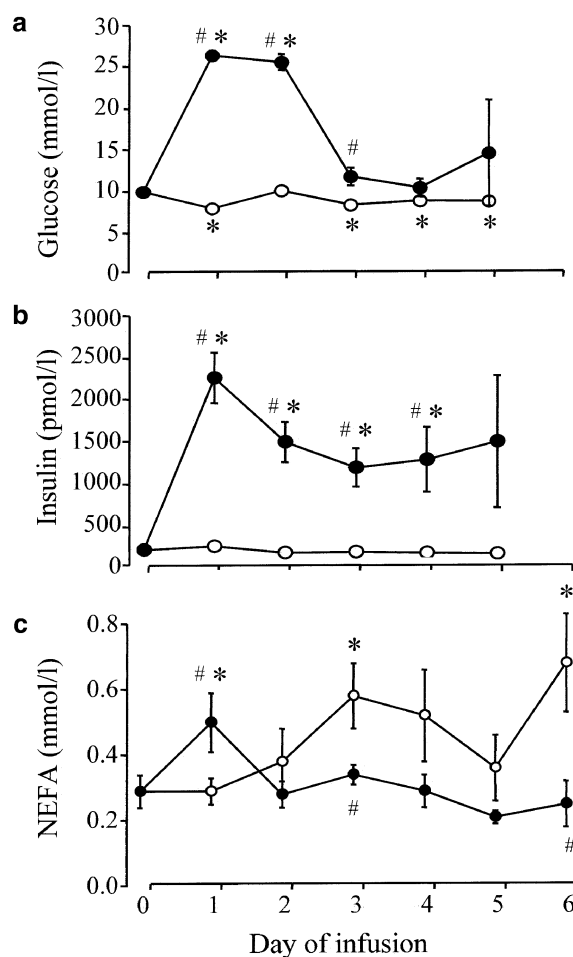


**Fig. 2.** Venous plasma glucose (a), insulin (b) and NEFA (c) levels in rats infused with saline (○) or glucose (●). #  $p < 0.05$  for comparison of the two groups; \*  $p < 0.05$  vs Day 0

$10.0 \pm 0.9$  mg on Day 6). Average beta cell size increased by approximately 25% between Days 1 and 3 of glucose infusion (Fig. 3). Replication rates, as assessed by BrdU incorporation, displayed a non-linear



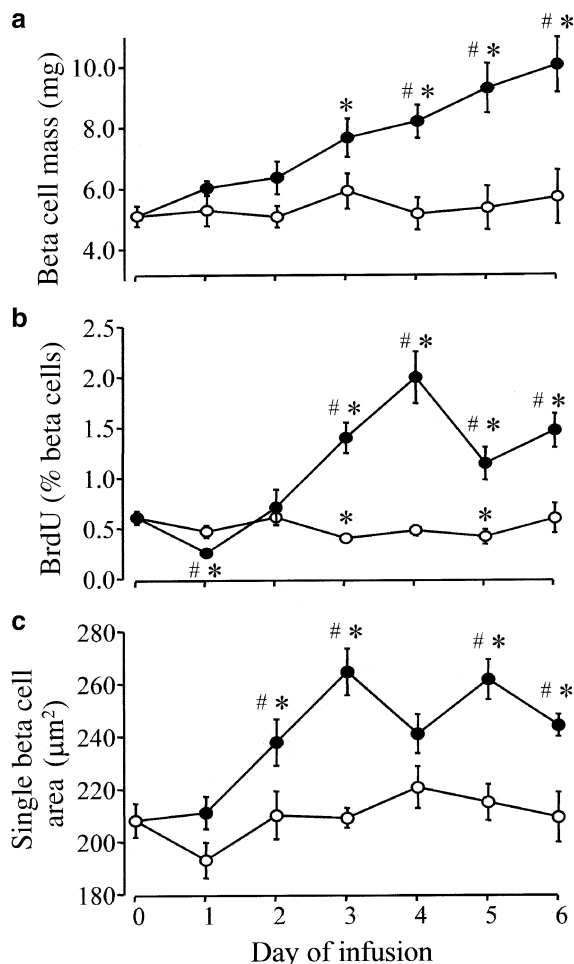


**Fig. 3.** Beta cell mass (a), BrdU incorporation into beta cells (b) and beta cell area (c) in rats infused with saline (○) or glucose (●). # $p < 0.05$  for comparison of the two groups; \* $p < 0.05$  vs Day 0

time course: rates decreased on Day 1, then increased until Day 4 and remained elevated on Days 5 and 6.

**$\beta$ IG model analysis.** In the saline group, insulin sensitivity remained statistically unchanged, but did display a trend towards an increase (Fig. 4). This result is consistent with modest decrease in glucose levels seen in the present study during a period of constant insulinaemia. While the dynamics of insulin sensitivity are reasonably intuitive in the saline group, the presence of a chronic glucose infusion complicates the calculation. However,  $\beta$ IG model analysis of these data suggests that glucose levels on Day 1 and Day 2 of infusion are higher than can be accounted for by the chronic glucose infusion alone (given the observed degree of insulinaemia). This analysis suggests that whole-body insulin sensitivity decreased by approximately 80% on Day 1 in saline-infused rats. While it is clear that insulin sensitivity increases between Days 2 and 3 (as glucose levels drop dramatically while insulinaemia and infusion rates remain un-

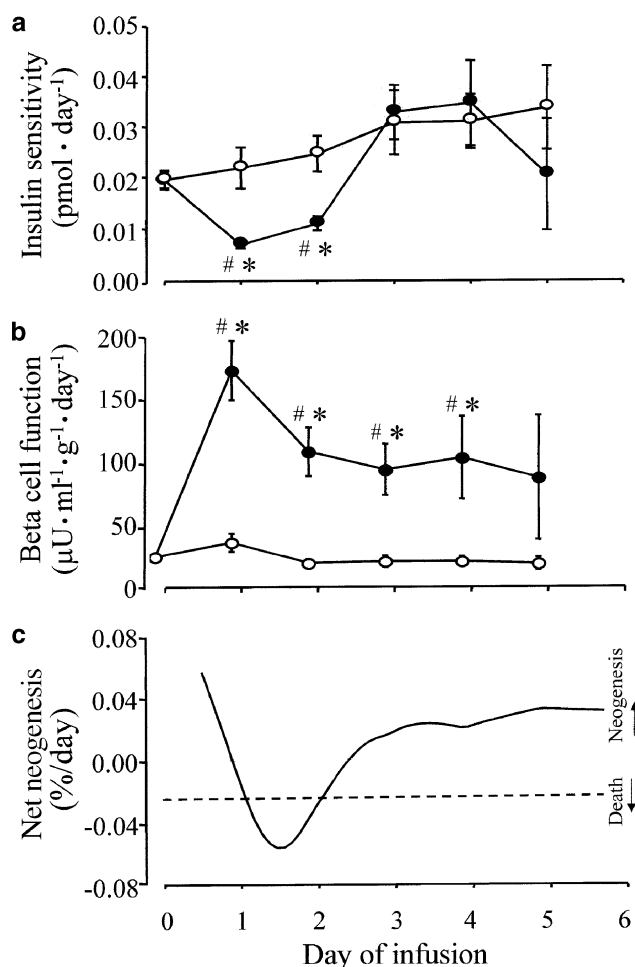


**Fig. 4.**  $\beta$ IG model-derived estimates of insulin sensitivity (a) and beta cell function (b) in rats infused with saline (○) or glucose (●). c. The  $\beta$ IG model estimates of net neogenesis are shown for rats infused with saline (dashed line) or glucose (solid line). # $p < 0.05$  for comparison of the two groups; \* $p < 0.05$  vs Day 0

changed), the magnitude of this change is non-intuitive. The  $\beta$ IG model analysis of these data suggests that during this period insulin sensitivity returns to the pre-infusion level and remains at this level for the remainder of the study.

The  $\beta$ IG model estimates of beta cell function for the two groups are presented in Figure 4. The estimates indicate whether the observed insulin levels are higher or lower than those expected for the prevailing values for glucose and beta cell mass in the two groups. The saline-infused animals displayed stable insulin levels, consistent with the relatively unchanged values observed for glucose levels and beta cell mass in these animals. Thus,  $\beta$ IG model analysis of these data suggests that beta cell function remains unchanged in the saline group. Conversely, the glucose-infused animals displayed hyperinsulinaemia beyond that predicted by the observed dynamics for glucose and beta cell mass alone. The  $\beta$ IG model analysis of this data suggests a transient increase (three- to four-fold) in beta cell function in these animals (Fig. 4).

The observation of constant beta cell mass in the presence of constant beta cell replication rates (~2% per day) in saline-infused animals clearly suggests that these animals display a constant rate of net neogenesis (neogenesis–death = –2% per day). Beta cell mass dynamics in the glucose-infused animals proved to be more complex. The data for beta cell mass, cell size and BrdU data were fitted using simple equations (linear, sigmoid and piecewise linear equations respectively), and the curve-fit data were subsequently used to estimate net neogenesis. Our calculations suggest glucose-infused rats display two waves of net neogenesis which are interrupted by a wave of net beta cell death (Fig. 4). Although we cannot calculate independent estimates for the rate of neogenesis or the rate of beta cell death, these data do suggest that each of the two waves of neogenesis must be no lower than 4% per day (as death rates are >0% per day). Similarly, the middle wave of beta cell death rates must incorporate death of at least 5% per day (as the neogenesis rate cannot be negative).

## Discussion

Humans and animals with Type 2 diabetes display insulin resistance, insulin secretory defects and insufficient (possibly reduced) beta cell mass [16, 17, 18, 19, 20]. Several authors have suggested that diabetes is characterised by insufficient beta cell adaptation to insulin resistance [15, 21, 22] followed by beta cell failure. While there is increasing evidence suggesting that glucose plays a critical role in beta cell failure [23, 24, 25, 26, 27], the role of glucose during the early phase of insufficient adaptation has been the subject of much debate. Some authors have proposed that glucose is the primary regulator of beta cell mass and function in vivo, whereas others have noted beta cell adaptation in the absence of hyperglycaemia [5, 6, 8, 10, 15, 28, 29, 30, 31, 32]. Several researchers have employed the chronic glucose infusion protocol to investigate the effects of chronic hyperglycaemia on beta cell mass, replication, death, neogenesis and function, and on peripheral insulin action [1, 2, 3, 5, 6, 7, 8, 10, 11, 25]. Due to the limitations of existing experimental techniques, these studies have each reported only a limited number of variables and time points.

In this study, we utilised quantitative morphology and mathematical modelling to estimate the full dynamical response of each of the physiological variables listed above during a chronic glucose infusion. Our findings were consistent with previous reports of transient insulin resistance and elevated beta cell function in vivo [3, 7]. We were also able to confirm the contributions of neogenesis, hypertrophy and hyperplasia in the early expansion of the beta cell mass in this protocol. Novel findings from this study include the  $\beta$ IG model prediction of increased beta cell death during

Day 2 of infusion and the existence of a second wave of beta cell neogenesis that occurs during the second half of the study. This predicted second wave of neogenesis is consistent with our previous finding of “focal” areas on Day 3 of chronic glucose infusion [33].

The predicted dynamics of whole-body insulin sensitivity reported here are consistent with previous animal studies that have addressed this issue. Laybutt and colleagues demonstrated that whole-body insulin sensitivity was reduced on Day 1 of glucose infusion, but normalised by Day 4 [3]. The initial insulin resistance has been shown to mainly be based in muscle and likely occurs as a direct result of the prevailing hyperglycaemia [2, 3, 34]. Later increases in insulin sensitivity are largely due to increased glucose uptake by adipose tissue [3, 4]. The mechanisms regulating this adaptation are not well understood. The similarity of our model predictions to data from the literature, coupled to the previous observation of a strong correlation between  $\beta$ IG model and Minimal model estimates of insulin sensitivity, suggests that the dynamics of insulin sensitivity reported here are accurate. Thus, while hyperglycaemia and hyperinsulinaemia have long been shown to cause insulin resistance [34, 35], the transient nature of this insulin resistance suggests that long-term insulin sensitivity may be regulated by adipose tissue physiology.

In this study, consistent with previous results, chronic glucose infusion led to persistent hyperinsulinaemia, despite the fact that the hyperglycaemia was observed to be transient. Previous studies on the contribution of beta cell function to this hyperinsulinaemia have produced conflicting results. Our findings are consistent with existing studies that have utilised in vivo methodologies to quantify beta cell function, but are in contrast with studies that have utilised in situ or in vitro methodologies to estimate glucose-induced insulin secretion [5, 6, 7, 8, 36, 37]. One animal study, in which both in vivo and in situ measurements of beta cell function were taken following 4 days of glucose infusion, found that insulin secretion was elevated in vivo but reduced in situ [37]. Discrepancy between in vitro and in vivo indices of beta cell function may be related to changes in beta cell function during the isolation process or to some other blood-borne secretagogue.

The observed rate of beta cell mass expansion in this study is similar to, or slower than, the rates reported in other chronic glucose infusion studies [6, 10, 11, 36]. Our beta cell replication and hypertrophy data are consistent with previous reports [10, 11, 36]. The early wave of beta cell neogenesis predicted in this study is also in agreement with a previous finding of neogenesis at 24 h but not at 48 h [10]. The prediction of a wave of beta cell death during the second day of infusion provides corroborating evidence for hyperglycaemia-induced apoptosis [38]. However, in contrast with our prediction, the results of a study by Bernard

et al. indicated a reduced number of TUNEL-positive beta cells on Day 1 and Day 2 of glucose infusion [10]. Firstly, it should be noted that both this study and the present study reported increasing replication, increasing cell size and a relatively constant beta cell mass during the second day of infusion. These data intuitively suggest increased beta cell death during this period. Secondly, given that our predicted wave of apoptosis was highly transient and peaked at 36 h, and that Bernard et al. quantified TUNEL-positive beta cells at 24 h and 48 h, it is possible that this brief wave was not detected in the latter study. It is also important to remember that these two methods provide different indices of cell death, which are subject to different potential sources of error. In the  $\beta$ IG model, errors or biases in beta cell mass and replication affect the estimate of beta cell death, whereas use of the TUNEL method as an index of the rate of beta cell death is based on the assumption that the clearance of the apoptotic cells is not affected by the treatment [39]. Finally, this discrepancy may simply reflect differences in animal models (adult Wistar rat versus young Sprague–Dawley rat). Further investigation is necessary if this difference is to be resolved.

Our model-based analysis of beta cell mass dynamics predicted a second wave of beta cell neogenesis between Day 3 and Day 6 of glucose infusion. This is consistent with our previous finding of “focal areas” on Day 3 of glucose infusion [33]. These areas, consisting of de-differentiated acinar tissue full of BrdU-positive cells and small amounts of insulin staining, are similar to those previously reported following a partial pancreatectomy [40]. Together, these data suggest a potentially important contribution of acinar-to-islet transdifferentiation to the beta cell mass adaptation that occurs during chronic glucose infusion.

In summary, by employing a combined mathematical and experimental approach we have performed the most complete analysis of the metabolic adaptation to chronic glucose infusion to date. The results confirm previous reports of transient insulin resistance, elevated in vivo beta cell function and an early wave of neogenesis. Our finding of a second wave of neogenesis provides further support for our previous hypothesis of a late wave of acinar-to-islet transdifferentiation. Overall, the agreement between  $\beta$ IG model predictions and the prevailing literature suggests that this methodology may provide a practical and reliable means of performing integrative and dynamic analysis of metabolic adaptation.

*Acknowledgements.* These studies were supported by a grant from the Canadian Institutes of Health Research (CIHR, MT10574). B. G. Topp is funded by the Canadian Diabetes Association, Florence L. Cotton memorial studentship and the centre for Mathematics of Information Technology and Complex Systems. The authors are grateful for the technical assistance of M. J. Thomas, D. Tzur, A. Dunichand-Hoedl, W. E. Fieldus, N. Dhatt, J. T. Lewis, G. LaChance, J. Trudeau, D. Crouch, J. Przydziecki and S. G. Chadan.

## Appendix

The equations for the  $\beta$ IG model (augmented to include exogenous glucose supply) are as follows:

$$dG/dt = R_0 - (E_0 + S_I I)G + G_{inf} \quad (1)$$

$$dI/dt = \beta\sigma G^2 / (\alpha^2 + G^2) - kI \quad (2)$$

$$d\beta_n/dt = (\text{Replication} - \text{Death} + \text{Neogenesis})\beta_n \quad (3)$$

$\alpha$ , sensitivity of insulin secretion to glucose (half max);  $\beta$ , beta cell mass;  $\beta_n$ , beta cell number;  $\sigma$ , maximal rate at which a single beta cell can secrete insulin;  $E_0$ , glucose effectiveness at zero insulin;  $G$ , plasma glucose;  $G_{inf}$ , glucose infusion rate;  $I$ , plasma insulin;  $k$ , insulin clearance constant;  $R_0$ , hepatic glucose production at zero insulin;  $S_I$ , insulin sensitivity;  $t$ , time. Full development of these equations has been described previously [15].

*Estimation of insulin sensitivity.* Mean insulin sensitivity was calculated from equation (1) using mean glucose and insulin values for each group at each time point by assuming: (i)  $dG/dt=0$  at the time of the sample; and (ii) a constant, error-free value for  $R_0$  and  $E_0$ . The standard error of the estimate of insulin sensitivity in each group at each time point was calculated by the Taylor expansion method of equation (1) incorporating the standard errors of the glucose and insulin measurements.

$$S_I = (R_0 - EG + G_{inf}) / (GI) \quad (4)$$

*Estimation of beta cell function.* Beta cell function ( $\sigma$ ) was calculated from equation (2) using mean glucose, insulin and beta cell mass values for each group at each time point assuming: (i)  $dI/dt=0$  at the time of the sample, and (ii) a constant, error-free value for  $\alpha$  and  $k$ . Again, the standard error of the estimate of beta cell function in each group at each time point was calculated by the Taylor expansion method of equation (2) incorporating the standard errors of the glucose, insulin and beta cell mass measurements.

$$\sigma = kI(\alpha^2 + G^2) / (\beta G^2) \quad (5)$$

*Estimation of net neogenesis.* Since equation (3) contains an implicit assumption of constant size of individual beta cells, calculation of net neogenesis required the incorporation of cell size to equation (3). Briefly, beta cell mass ( $\beta$ ) is dependent on the number ( $\beta_n$ ) and the size of pancreatic beta cells ( $\beta_s$ ):

$$\beta = (\beta_s)(\beta_n) \quad (6)$$

The rate of change ( $d/dt$ ) of beta cell mass can be expressed as a chain rule expansion of equation (6):

$$d\beta/dt = (d\beta_s/dt)(\beta_n) + (d\beta_n/dt)(\beta_s) \quad (7)$$

Dividing through by  $\beta$  and substituting in equation (3) for the rate of change of beta cell number, we arrive at:

$$\frac{d\beta/dt}{\beta} = \frac{d\beta_s/dt}{\beta_s} + \text{Replication} - \text{Death} + \text{Neogenesis} \quad (8)$$

Since net neogenesis (neogenesis–death) occurs on the same time scale as the dynamics of beta cell mass and beta cell size, one can not assume  $d\beta/dt=0$  or  $d\beta_s/dt=0$ .

$$\text{Net neogenesis} = \frac{d\beta/dt}{\beta} - \frac{d\beta_s/dt}{\beta_s} - \text{Replication} \quad (9)$$

The dynamics of  $\beta$ ,  $d\beta/dt$ ,  $\beta_s$  and  $d\beta_s/dt$  were determined via simple curve fits (non-linear least squares algorithm; MLAB, Civilized Software, Silver Spring, Md., USA) of beta cell mass and beta cell size data. Since BrdU labels beta cells entering into S-phase during a 6-h window, beta cell replication rates (% per day) were assumed to be four times the percentage of BrdU positive beta cells. Replication rate data from the saline-infused group were fitted with a simple linear equation; however, the dynamics of beta cell replication in the glucose-infused animals was complex and could not be fitted well by any simple polynomial or sigmoid equation. Thus, replication rates from this group were determined by an optimal segments smoothing algorithm.

**Normal parameter values.** The normal, rat-specific parameter values used in this study are [15]:  $R_0=49.6 \text{ mmol}\cdot\text{l}^{-1}\cdot\text{day}^{-1}$ ,  $E=1.44 \text{ per day}^{-1}$ ,  $\alpha=61.6 \text{ mmol}^2\cdot\text{l}^{-2}$ ,  $k=432 \text{ day}^{-1}$ ,  $G_{\text{inf}}=579 \text{ mmol}\cdot\text{l}^{-1}\cdot\text{day}^{-1}$  based on 50% dextrose infusion at 2 ml/h and an assumed 25% of mass glucose volume of distribution space.

## References

- Leahy JL, Cooper HE, Deal DA, Weir GC (1986) Chronic hyperglycemia is associated with impaired glucose influence on insulin secretion. A study in normal rats using chronic in vivo glucose infusions. *J Clin Invest* 77:908–915
- Hager SR, Jochen AL, Kalkhoff RK (1991) Insulin resistance in normal rats infused with glucose for 72 h. *Am J Physiol Endocrinol Metab* 260:E353–E362
- Laybutt DR, Chisholm DJ, Kraegen EW (1997) Specific adaptations in muscle and adipose tissue in response to chronic systemic glucose oversupply in rats. *Am J Physiol Endocrinol Metab* 273:E1–E9
- Takao F, Laury MC, Ktorza A, Picon L, Penicaud L (1990) Hyperinsulinaemia increases insulin action in vivo in white adipose tissue but not in muscles. *Biochem J* 15:255–257
- Bedoya F, Jeanrenaud B (1991) Evolution of insulin secretory response to glucose by perfused islets from lean (Fa/Fa) rats chronically infused with glucose. *Diabetes* 40:7–14
- Bernard C, Thibault C, Berthault MF et al. (1998) Pancreatic  $\beta$ -cell regeneration after 48-h glucose infusion in mildly diabetic rats is not correlated with functional improvement. *Diabetes* 47:1058–1065
- Kuboi M, Egawa M, Udaka N, Ito T, Inoue S, Sekihara H (1998) Effects of a 7-day infusion of glucose on insulin secretion in vivo and in vitro ventromedial hypothalamic-lesioned obese rats. *Acta Diabetol* 35:26–33
- Leahy JL, Cooper HE, Weir GC (1987) Impaired insulin secretion associated with near normoglycemia. Study in normal rats with 96-h in vivo infusions. *Diabetes* 36:459–464
- Sako Y, Grill VE (1990) Coupling of beta-cell desensitization by hyperglycemia to excessive stimulation and circulating insulin in glucose-infused rats. *Diabetes* 39:1580–1583
- Bernard C, Berthault MF, Saulnier C, Ktorza A (1999) Neogenesis vs. apoptosis as main components of pancreatic  $\beta$ -cell mass changes in glucose-infused normal and mildly diabetic adult rats. *FASEB J* 13:1195–1205
- Bonner-Weir S, Deery D, Leahy JL, Weir GC (1989) Compensatory growth of pancreatic  $\beta$ -cells in adult rats after short-term glucose infusion. *Diabetes* 38:49–53
- Matthews DR, Hosker JP, Rudenski AS et al. (1985) Homeostasis model assessment: insulin resistance and beta-cell function from fasting plasma glucose and insulin concentrations in man. *Diabetologia* 28:412–419
- Katz A, Nambi SS, Mather K et al. (2000) Quantitative insulin sensitivity check index: a simple, accurate method for assessing insulin sensitivity in humans. *J Clin Endocrinol Metab* 85:2402–2410
- Finegood DT, Scaglia L, Bonner-Weir S (1995) Dynamics of beta-cell mass in the growing rat pancreas. Estimation with a simple mathematical model. *Diabetes* 44:249–256
- Topp BG, Promislow K, de Vries G, Miura RM, Finegood DT (2000) A model of  $\beta$ -cell insulin, and glucose kinetics: pathways to diabetes. *J Theor Biol* 206:605–619
- Pick A, Clark J, Kubstrup C et al. (1998) Role of apoptosis in failure of beta-cell mass compensation for insulin resistance and beta-cell defects in the male Zucker diabetic fatty rat. *Diabetes* 47:358–364
- Finegood DT, Topp BG (2001)  $\beta$ -cell deterioration—prospects for reversal or prevention. *Diabetes Obes Metab* 3 [Suppl 1]:S20–S27
- Kloppel G, Lohr M, Habich K, Oberholzer M, Heitz PU (1985) Islet pathology and the pathogenesis of type 1 and type 2 diabetes mellitus revisited. *Surv Synth Pathol Res* 4:110–125
- Leahy JL (1990) Natural history of  $\beta$ -cell dysfunction in NIDDM. *Diabetes Care* 13:992–1010
- Sakuraba H, Mizukami H, Yagihashi N, Wada R, Hanyu C, Yagihashi S (2002) Reduced  $\beta$ -cell mass and expression of oxidative stress-related DNA damage in the islet of Japanese Type II diabetic patients. *Diabetologia* 45:85–96
- Bergman RN, Finegood DT, Ader M (1985) Assessment of insulin sensitivity in vivo. *Endocr Rev* 6:45–58
- Cerasi E (1995) Insulin deficiency and insulin resistance in the pathogenesis of NIDDM: is a divorce possible? *Diabetologia* 38:992–997
- Poitout V, Robertson RP (2002) Secondary  $\beta$ -cell failure in type 2 diabetes—a convergence of glucotoxicity and lipotoxicity. *Endocrinol* 143:339–342
- Rossetti L (1995) Glucose toxicity: the implications of hyperglycemia in the pathophysiology of diabetes mellitus. *Clin Invest Med* 18:255–260
- Unger RH, Grundy S (1985) Hyperglycemia as an inducer as well as a consequence of impaired islet cell function and insulin resistance: implications for the management of diabetes. *Diabetologia* 28:119–121
- Unger RH (2002) Lipotoxicity diseases. *Annu Rev Med* 53:319–336
- Weir GC, Laybutt DR, Kaneto H, Bonner-Weir S, Sharma A (2001) Beta-cell adaptation and decompensation during the progression of diabetes. *Diabetes* 50 [Suppl 1]:S154–S159



28. Efanova IB, Zaitsev SV, Zhivotovsky B et al. (1998) Glucose and tolbutamide induce apoptosis in pancreatic  $\beta$ -cells. *J Biol Chem* 273:33501–33507
29. Hugl SR, White MF, Rhodes CJ (1998) Insulin-like growth factor I (IGF-I)-stimulated pancreatic  $\beta$ -cell growth is glucose-dependent. *J Biol Chem* 273:17771–17779
30. Hoorens A, Van de Casteele M, Kloppel G, Pipeleers D (1996) Glucose promotes survival of rat pancreatic  $\beta$ -cells by activating synthesis of proteins which suppress a constitutive apoptotic program. *J Clin Invest* 98:1568–1574
31. Liu YQ, Montanya E, Leahy JL (2001) Increased islet DNA synthesis and glucose-derived lipid and amino acid production in association with beta-cell hyperproliferation in normoglycaemic 60% pancreatectomy rats. *Diabetologia* 44:1026–1033
32. Swenne I (1982) The role of glucose in the in-vitro regulation of cell cycle kinetics and proliferation of fetal pancreatic  $\beta$ -cells. *Diabetes* 31:754–760
33. Lipsett M, Finegood DT (2002)  $\beta$ -cell neogenesis during prolonged hyperglycemia in rats. *Diabetes* 51:1834–1841
34. Unger RH, Grundy S (1985) Hyperglycemia as an inducer as well as a consequence of impaired islet cell function and insulin resistance: implications for the management of diabetes. *Diabetologia* 28:119–121
35. Pirola L, Bonnafous S, Johnston AM, Chaussade C, Portis F, Van Obberghen E (2003) Phosphoinositide 3-kinase-mediated reduction of IRS-1/2 protein expression via different mechanisms contributes to the insulin-induced desensitization of its signaling pathways in L6 muscle cells. *J Biol Chem* 278:15641–15651
36. Steil GM, Trivedi N, Jonas JC et al (2001) Adaptation of beta-cell mass to substrate oversupply: enhanced function with normal gene expression. *Am J Physiol Endocrinol Metab* 280:E788–E796
37. Laury MC, Takao F, Bailbe D et al (1991) Differential effects of prolonged hyperglycemia on in vivo and in vitro insulin secretion in rats. *Endocrinology* 128:2526–2533
38. Maedler K, Sergeev P, Ris F et al. (2002) Glucose-induced beta cell production of IL-1 $\beta$  contributes to glucotoxicity in human pancreatic islets. *J Clin Invest* 110:851–860
39. O'Brien BA, Fieldus WE, Field CJ, Finegood DT (2002) Clearance of apoptotic beta-cells is reduced in neonatal autoimmune diabetes-prone rats. *Cell Death Differ* 9:457–464
40. Bonner-Weir S, Baxter LA, Schuppin GT, Smith FE (1993) A second pathway for regeneration of adult exocrine and endocrine pancreas. A possible recapitulation of embryonic development. *Diabetes* 42:1715–1720